THE JOURNAL OF PHYSICAL CHEMISTRY B

Article

pubs.acs.org/JPCB

Short Hydrogen Bonds and Negative Charge in Photoactive Yellow Protein Promote Fast Isomerization but not High Quantum Yield

Jingyi Zhu,[†] Jocelyne Vreede,[‡] Marijke Hospes,[§] Jos Arents,[§] John T. M. Kennis,[†] Ivo H. M. van Stokkum,[†] Klaas J. Hellingwerf,[§] and Marie Louise Groot*[,†]

[†]Department of Physics and Astronomy, Faculty of Sciences, LaserLab, VU University Amsterdam, De Boelelaan 1081, 1081 HV Amsterdam, The Netherlands

[‡]Van't Hoff Institute for Molecular Sciences and [§]Laboratory for Microbiology, Swammerdam Institute for Life Sciences, University of Amsterdam, Science Park 904, 1098 XH Amsterdam, The Netherlands

Supporting Information

ABSTRACT: Biological signal transduction by photoactive yellow protein (PYP) in halophilic purple sulfur bacteria is initiated by trans-to-cis isomerization of the *p*-coumaric acid chromophore (pCa) of PYP. pCa is engaged in two short hydrogen bonds with protein residues E46 and Y42, and it is negatively charged at the phenolate oxygen. We investigated the role in the isomerization process of the E46 short hydrogen bond and that of the negative charge on the anionic phenolate moiety of the chromophore. We used wild-type PYP and the mutant E46A, in protonated and deprotonated states (referred to as pE46A and dpE46A, respectively), to reduce the number of hydrogen bond interactions between the pCa phenolate oxygen and the protein and to vary the negative charge density in the chromophore-binding pocket. Their effects on the yield and rate of chromophore isomerization were determined by ultrafast spectroscopy. Molecular dynamics simulations were used to relate these results to structural changes in the mutant protein. We found that deprotonated pCa in E46A has a slower isomerization rate as the main part of this reaction was associated with time constants of 1 and 6 ps, significantly slower than the 0.6 ps time constant in wild-type PYP. The quantum yield of isomerization in dpE46A was estimated to be 30 ± 2%, and that of pE46A was 32 ± 3%, very close to the value determined for wtPYP of 32 ± 2%. Relaxation of the isomerized product state I_0 to I_1 was faster in dpE46A. We conclude that the negative charge on pCa stabilized by the short hydrogen bonds with E46 and Y42 affects the rate of isomerization but not the quantum yield of isomerization. With this information, we propose a scheme for the potential energy surfaces involved in the isomerization and suggest protein motions near the pCa backbone as key events in successful isomerization.

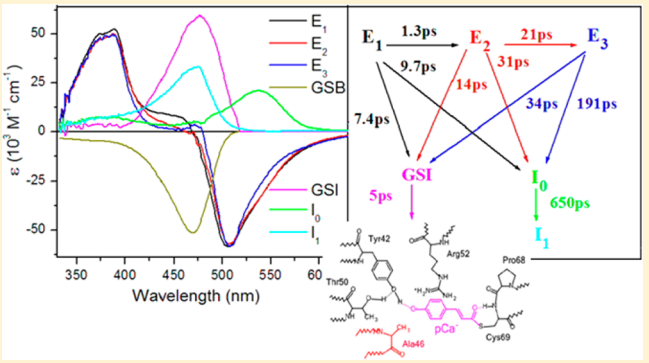

INTRODUCTION

Photoactive yellow protein (PYP) is a blue-light photoreceptor that is responsible for the negative phototaxis in halophilic purple sulfur bacteria.[1−3] The functional chromophore inside PYP is a deprotonated *trans*-*p*-hydroxycinnamic acid (*p*-coumaric acid, pCa), covalently linked to the protein via the side chain of a cysteine residue (C69) by a thioester bond (Figure 1). In wild-type (wt) PYP at physiological pH, the pCa chromophore is deprotonated and forms part of a hydrogen bond (HB) network, which connects the amino acid residues E46 and Y42 to the phenolate oxygen of the pCa chromophore in the active site and its carbonyl oxygen to the backbone NH group of C69. Upon absorption of blue light, pCa isomerizes from the trans to cis configuration around the $C_7{=}C_8$ double bond, with a quantum yield of about 0.3 within a few picoseconds, forming a photocycle intermediate denoted I_0.[4−15] Relaxation of the pCa backbone occurs in about 1 ns, thus forming a state denoted I_1. Later in the photocycle, proton transfer to the chromophore takes place, followed by a partial unfolding of the protein on a millisecond time scale.[16,17] In solution and in the denatured protein, instead of forming stable photoisomerized cis products, the photoreaction of the pCa chromophore results in twisted trans conformations that relax back to the trans ground state or, at higher excitation densities, in photoionization of the chromophore.[18,19]

Remarkable structural features of the PYP protein are the negative charge on the phenolate oxygen of the chromophore, inside of the chromophore-binding pocket, and the nature of the HBs of the phenolate oxygen with residues E46 and Y42. In the ground-state structure of PYP, pCa is in its anionic form, with a negative charge on the phenolic oxygen.[20,21] This

Special Issue: Photoinduced Proton Transfer in Chemistry and Biology Symposium

Received: July 8, 2014
Revised: August 20, 2014
Published: August 21, 2014

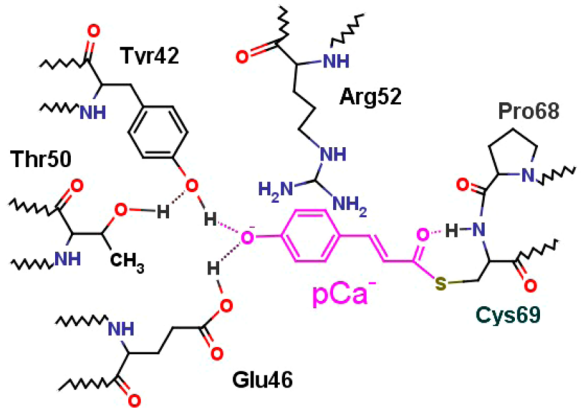

Figure 1. Representation of the pCa chromophore and active site amino acid residue structures in wtPYP.

negative charge has been suggested to play a role in the charge redistribution in the chromophore of PYP, upon formation of the electronically excited singlet state through absorption of a blue photon, as deduced from results obtained with Stark spectroscopy.[22] This charge redistribution was suggested to consist of migration of the negative charge on the phenolic oxygen toward the thioester linkage, giving the double bond of the hydrogen-bonded carbonyl group more of a single-bond character, thereby lowering the barrier for isomerization.[22−26]

In general, an isolated charge buried in a protein's interior will destabilize the protein structure; to be electrically neutralized, it must be able to couple with a counterion. The counterion against pCA's negative charge was thought to be the cationic form of R52 at a distance of 6.34 Å from the phenolic oxygen of pCA.[27] Experiments in which R52 was targeted in different ways[11,28] revealed that the net charge of R52 does not significantly influence the primary photochemistry of PYP. This is in good agreement with recent neutron diffraction experiments that indeed show that R52 is neutral rather than charged.[29] It therefore appears that the negative charge on pCa is stabilized solely by the HBs with E46 and Y42.[29]

The HBs that the phenolic oxygen accepts from E46 and Y42 are very short. X-ray crystallographic studies of PYP with better than 1.0 Å resolution[30−32] revealed 2.5−2.6 Å oxygen−oxygen distances for the HBs donated by Y42 and E46, respectively. Normal HBs display bond lengths of 0.95 Å for the donor O−H bond and about 2.07 Å for the H-acceptor bond, resulting in an average O to O distance of 3.02 Å.[29] QM/MM simulations[23−26] suggest that the HBs of the phenolic oxygen to Y42 and E46 are the crucial factor for the ultrafast decay from the twisted double-bond minimum and formation of the isomerized chromophore. Furthermore, E46 is conserved in almost all variants of PYP.[33]

In earlier studies, the rigidity of the HBs and of the protein nanospace were modified by point mutations to residues E46, Y42, and T50.[9,34−37] The HB coordination of the chromophore phenolate group was weakened or deleted by mutations to E46 and Y42, while the slightly more distant HB between T50 and Y42 was weakened in T50V. Mutations were observed to increase the excited-state lifetime, shift the absorption maximum of pCa, and loosen the protein nanospace.[9,34,35] The HB network around the chromophore was concluded to be important for stabilization of the chromophore's negative charge and tuning of its absorption maximum in the ground state.[9,36,37] Also, from analyzing a range of E46 mutants, the low fluorescence quantum yield of wtPYP was concluded to have been selected for during evolution. The biological relevance of the low fluorescence quantum yield was rationalized by assuming it to be correlated with a high quantum yield for photochemistry.[37]

Here, we addressed the question if and how the negative charge on the phenolic oxygen and the short HBs between the phenolic oxygen and the protein influence the isomerization quantum yield. Do the short HBs with E46 and Y42 serve to stabilize the electron on a specific location, such that upon light absorption by pCa, a charge redistribution is created that leads to isomerization with a high quantum yield? We have compared results from femtosecond visible pump−probe spectroscopy obtained on wtPYP with those of the mutant E46A, with its chromophore in protonated and deprotonated states. By replacing E46 with alanine, the HB with residue 46 was eliminated,[38] and by protonation of the phenolic oxygen, the HB acceptor capabilities of the phenolic oxygen were restricted. Accordingly, we expected the two HBs to be stepwise eliminated. In addition, in this set of samples, the charge density on the phenolic oxygen was varied, from a higher negative charge density in deprotonated E46A, via wt, to no negative charge density in protonated E46A. This allowed us to investigate the effect of both the short HBs and the negative charge density on the phenolic oxygen on the isomerization rate and quantum yield.

For wtPYP, the pK_a of the chromophore is around 2.8;[39,40] thus, in the physiological range (pH ≈ 5−9), only the deprotonated form exists. However, for the mutant E46A, due to the higher pK_a value (pK_a ≈ 7.8/7.9[41,42]) at neutral pH, two forms of the chromophore coexist, proteins with deprotonated pCa and with protonated pCa. This situation thus provides an opportunity to investigate the HB network inside of PYP under nondenaturing conditions by tuning of the excitation wavelength. We will refer to the deprotonated E46A as dpE46A, to the protonated E46A as pE46A, and to the wtPYP with a deprotonated chromophore as wtPYP in the following. Figure 1 depicts the molecular structure of wtPYP. We performed molecular dynamics (MD) simulations for all three types of PYP to determine the HB network in the three samples and to relate their differences to the results of the transient absorption measurements.

MATERIALS AND METHODS

Site-directed mutagenesis was performed using the QuikChange kit (Stratagene, La Jolla, CA) and confirmed by DNA sequencing, as described previously.[43] The wtPYP and the site-directed mutant E46A were produced and isolated as described previously for wtPYP.[44] Apo-PYP was reconstituted with the 1,1′-carbonyldiimidazole derivative of *p*-coumaric acid chromophore, as described by Hendriks et al.[45] The reconstituted holoproteins were purified in two subsequent steps, with Ni affinity and anion exchange chromatography, respectively. The purified holoproteins were used without removal of the genetically introduced N-terminal hexahistidine-containing tag in a buffer containing 20 mM Tris pH 8.1.

Ground-state absorption spectra of all of the PYPs were recorded by a UV/vis spectrophotometer (Cary 4000). Steady-state fluorescence spectra were measured with a spectrophotometer (Jobin Yvon, Fluorolog) using 440 nm excitation for wtPYP, 460 nm for dpE46A, and 350 nm for pE46A, all with excitation band-pass filters of around 3 nm.

dx.doi.org/10.1021/jp506785q | J. Phys. Chem. B 2015, 119, 2372−2383

Ultrafast time-resolved spectra were recorded with a newly reconstructed femtosecond laser system, which will be described in more detail elsewhere. A Ti:sapphire oscillator (MaiTai, Spectra Physics) provided ~89 MHz pulse trains, with pulse width of ~30 fs. This oscillator beam was used to seed a regenerative amplifier (Hurricane, Spectra Physics) operating at 1 kHz. The amplifier had an output of ~0.6 mJ/pulse and a pulse width of ~100 fs. The output of the laser was sent to an optical parametric amplifier (TOPAS, Coherent), which was tuned to the desired wavelength for excitation of each of the samples. For excitation of dpE46A, the wavelength was set to 480 nm, with a pulse energy of 150 nJ. For excitation of pE46A, the 650 nm output of the TOPAS was frequency doubled to 325 nm with a 1 mm thickness $LiIO_3$ crystal. To decrease two-photon ionization of the chromophore by the UV photons while still maintaining a sufficient signal-to-noise ratio (S/N), an excitation energy of 50 nJ/pulse was used. For excitation of wtPYP, the output at 900 nm from the TOPAS was again frequency doubled to 455 nm with a 0.5 mm BBO crystal, and a pulse energy of 70 nJ was used. To generate a smooth supercontinuum probe pulse, the fundamental 800 nm was focused to a laterally rotating 2 mm thickness CaF_2 plate. After interrogation of the sample, the supercontinuum was dispersed in a spectrograph and detected on a 2064 channel CCD array (model S11155-2048; Hamamatsu).

PYP samples were held in a fused silica sample cell with a 1 mm optical path length and circulated with a peristaltic pump. The sample was refreshed at every laser shot. The integrity of the sample was determined by measuring its absorption spectrum before and after each run, and no deterioration was observed. The polarization of the probe pulse was set at the magic angle with respect to the excitation pulse. After a time-zero correction of the transient spectra for the group delay dispersion of the probe continuum, the data were analyzed with a kinetic model-based global fitting program.[46−51] Details of the method and program used are included in the Supporting Information.

The MD simulations were performed using GROMACS, version 4.5.5,[52,53] using the AMBER-03 force field[54] with TIP3P water.[55] The starting conformation for wtPYP was obtained from the atomic resolution crystal structure of the dark state (PDB code 1NWZ[31]), and for the E46A mutant, Glu46 was changed into alanine by deleting side-chain atoms. We performed simulations for three systems, wtPYP, dpE46A, and pE46A. The first two systems contained a deprotonated chromophore, and in the last system, the chromophore was protonated at the phenolate oxygen. Force field parameters for the chromophore in protonated and deprotonated configurations were kindly provided by G. Groenhof.

The structures were placed in a periodic dodecahedron box, filled with TIP3P water[55] after adding hydrogen atoms to all conformations. Protonatable groups were considered to be at neutral pH. For Arg52, we assumed that the pK_a would be close to the pK_a of arginine in water and was therefore protonated (resulting in a charge of +1 on this residue) at neutral pH. At lower pH, Arg52 was also protonated. Specific protons were added to Glu46 in the wtPYP system and to pCa at the phenolate oxygen in the pE46A system. Water molecules overlapping with the protein were removed, as well as waters not hydrogen bonding to the bulk. The charge of −6 on the protein was neutralized by adding 150 mmol/L of NaCl, corresponding to 16 Na^+ and 10 Cl^- ions. The resulting systems were then energy minimized using the conjugate gradient method. Then, the positions and velocities of the hydrogen atoms and water molecules were equilibrated for 10 ps at 300 K and 1 bar, while the protein heavy atoms were position restrained. After release of the restraints on the protein atoms, the systems were equilibrated for 50 ns, followed by 55 ns of sampling, saving coordinates every 2 ps. The temperature was kept constant at 300 K using the velocity-rescaling thermostat,[56] while the pressure remained constant at 1 bar with the use of the Parrinello−Rahman barostat.[57] Nonbonded interactions were treated with a cutoff at 1.1 nm, while long-range electrostatics were treated with PME.[58,59] All bonds were constrained using the LINCS algorithm[60] and SETTLE for water,[61] allowing for a time step of 2 fs. From the resulting trajectories, we calculated several distances and the number of water molecules around a residue using a combination of GROMACS tools and perl scripts. The simulations were performed on the Dutch National Compute Cluster LISA.

RESULTS AND ANALYSIS

Steady-State Spectra. Figure 2 presents the steady-state absorption and fluorescence emission spectra of wtPYP and the two E46A variants in 20 mM Tris buffer at pH 8.1. The bands at 275 nm are due to the apoprotein. The two bands at 350 and 470 nm in the spectrum of E46A (green line) arise from the chromophore pCa electronic transition to the lowest excited state. Their copresence indicates that at this pH, in the E46A mutant, the pCa chromophore can be protonated (pE46A, 350 nm) as well as deprotonated (dpE46A, 470 nm). The mutation

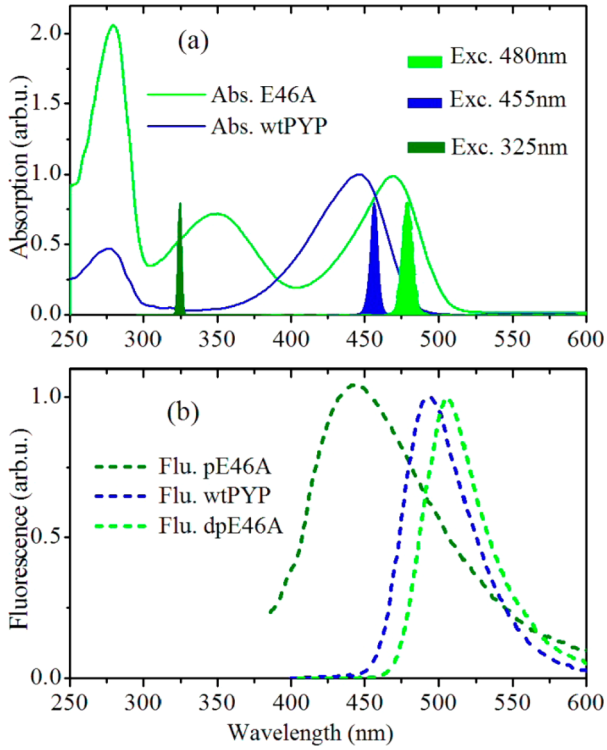

Figure 2. Steady-state absorption and fluorescence emission spectrum of wtPYP and mutant E46A at pH 8.1. (a) Absorption spectra and excitation wavelengths for the ultrafast transient absorption measurements of each sample. The filled areas are the excitation pulses centered at 325 nm for pE46A, 455 nm for wtPYP, and 480 nm for dpE46A, respectively. (b) Steady-state fluorescence emission spectra of the same three PYP samples.

dx.doi.org/10.1021/jp506785q | J. Phys. Chem. B 2015, 119, 2372−2383

therefore resulted in a significant increase of the pK_a. The λ_{max} value of pCa in dpE46A was red-shifted by about 25 nm in comparison to the 445 nm value of wtPYP, signaling an increase of the anionic character of the chromophore phenolate oxygen as a result of the loss of the HB with residue 46[37,38,62] or as a result of weakening of the HBs between pCa and the protein. For pE46A, the absorption was not only blue-shifted to λ_{max} = 350 nm due to protonation of the chromophore, but the absorption band was also much broader, with a fwhm of 6430 cm^{-1}, whereas that at 470 nm was 2480 cm^{-1}. The pH-dependent absorption spectra of E46A are provided in Figure S1 (Supporting Information). Similar to the absorption spectra, the fluorescence spectra were also red and blue-shifted, respectively, as can be seen in Figure 2b, but the size of the shift was smaller. The fluorescence emission spectrum of pE46A was also significantly broader than those of dpE46A and wtPYP. The broadening of the absorption and emission spectra of pE46A is a strong indication that, due to the protonation of the pCa and the resulting loss of HB(s), the flexibility of the phenol ring is greatly enhanced. Conversely, the similarity in the width of the spectra of wtPYP and dpE46A suggests that the flexibility of the phenol ring is restricted in both proteins and thus that the HB network in dpE46A may be largely intact, even though HB donor E46 was deleted. To investigate which changes in the HB network were induced by the E46A mutation and by the protonation of the chromophore, we performed MD simulations for all three proteins.

MD Simulations. In order to study in detail how the HB network adjusted to this mutation and the protonation of pCa, MD simulations were performed. The simulation results of wtPYP, dpE46A, and pE46A are depicted in Figure 3, with the variations of the length in the HBs formed between the chromophore and Y42, E46, and T50. Several previous studies indicated that the HBs between the phenolic oxygen of pCa (O4′) and E46 and Y42 are very short in wtPYP.[30−32] In agreement with that, the MD simulations reveal for wtPYP that oxygen O4′ accepts HBs from E46 and Y42. For E46 in wtPYP, the distance between O4′ and the hydrogen atom of E46 (HE2) is shorter than the average distance between an acceptor and the cognate hydrogen atom (2 Å) and can therefore be considered a short HB (26). In dpE46A, the HB of O4′ with Y42 is intact and shortened somewhat (Figure 3a), and a new HB is formed between the phenolic oxygen and T50 (Figure 3c). The shortening of the HB with Y42 is in good agreement with the observation of a strengthening of the HB with Y42 in the mutant E46Q by Sigala et al. with NMR.[63] In pE46A, pCa competes with T50 to be the HB donor to the backbone carbonyl oxygen of residue 46. When pCa forms a HB with the 46 backbone, T50 no longer participates in the HB network around pCa and also does not interact with Y42. When pCa interacts with the backbone, Y42 does not participate in any HBs. These interactions fluctuate at the subμs time scale (data not shown).

We conclude that pCa engages in two HBs in wtPYP and in dpE46A and in less than one in pE46A, in line with the observed broadening of the optical absorption and emission spectra.

Ultrafast Time-Resolved Spectra and Excited-States Dynamic. We next measured the ultrafast time-resolved absorption difference spectra to characterize excited-state decay processes and formation of the isomerized state in the wtPYP, dpE46A, and pE46A samples at pH 8.1. Representative time-dependent spectra are presented in Figure 4. For wtPYP

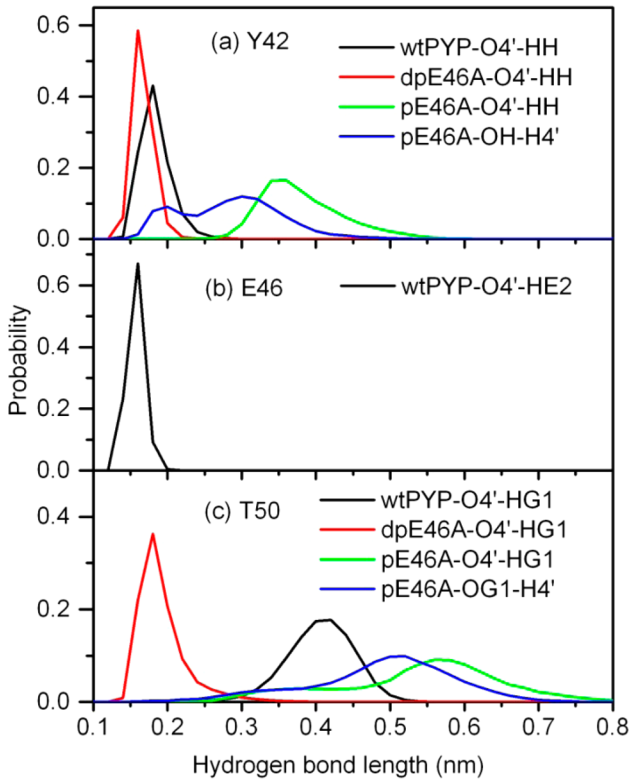

Figure 3. Distribution of HB distances involving pCa. O4′: phenol(ate) oxygen in pCa; H4′: phenolic hydrogen in protonated pCa; OH: phenolic oxygen in Y42; HH: phenolic hydrogen in Y42; HE2: hydrogen in E46; OG1: hydroxyl oxygen in T50; HG1: hydroxyl proton in T50. The bin size is 0.02 nm.

in panel (a) after excitation at 200 fs, an immediate buildup of signal consisting of excited-state absorption (380 nm), bleached ground-state absorption (450 nm), and stimulated emission (500 nm) was observed (black line). With increasing pump−probe delay time, the excited-state signals decayed and completely vanished after 40 ps, and the spectra evolved to the absorption−difference spectrum characteristic for the first cis product I_0, with its maximum absorption at around 520 nm (magenta line). The I_0 state relaxed to the I_1 state in about 2 ns, which had an absorption difference spectrum with a more blue-shifted maximum that mostly overlaps with the bleach signal (dark yellow line). These observations for wtPYP are consistent with those of previous measurements.[4−14,46]

In the transient spectra of dpE46A shown in Figure 4b, similarly, excited-state absorption, bleach, and stimulated emission signals were observed at early delay times. The bleach and stimulated emission were, however, more close and more overlapping with each other than those in wtPYP. Superimposed on these negative signals, a positive absorption-like signal at 490 nm was observed in the spectral evolution from 1 to 5 ps. This positive transient state most likely is the ground-state intermediate (GSI),[8,9] previously identified with wtPYP. The I_0 and I_1 absorption signatures in dpE46A were also similar to those in wtPYP but originated much later in time, and the I_1 absorption was hardly observable due to severe overlap with the bleach in the wavelength region at around 500 nm.

The transient spectra of pE46A, shown in Figure 4c, were at early delay times dominated by strong excited-state absorption on the blue side of the spectra and by stimulated emission on

dx.doi.org/10.1021/jp506785q | J. Phys. Chem. B 2015, 119, 2372−2383

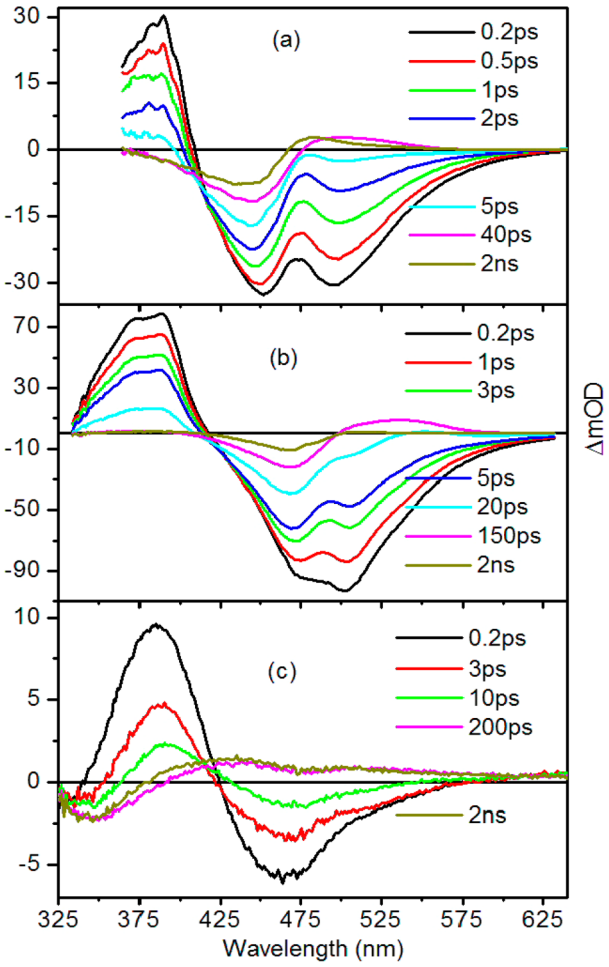

Figure 4. Dispersion-corrected transient difference spectra of the three PYP samples at selected delay times. (a) wtPYP; (b) dpE46A; (c) pE46A.

the red side of the spectra. The bleach signals were almost completely canceled by the strong excited-state absorption signal; only a very small negative signal can be distinguished at wavelengths below 330 nm. The stimulated emission band, with a maximum peak at around 470 nm, was much broader than those observed in wtPYP and dpE46A, consistent with the steady-state fluorescence measurements presented in Figure 2b. Product formation was observed, in agreement with an earlier report on pE46A,[38] on a time scale very similar to that in dpE46A. However, a striking difference was that only one product state was formed, whose shape did not evolve in time; compare the magenta and dark yellow curves in Figure 4c. Given its red-shifted position with respect to the ground-state absorption, we tentatively identify this product as a protonated I_1 cis isomer state. Apparently, in the protonated sample pE46A, either the relaxation of the photoisomerized I_0 product state to I_1 is too slow and falls outside of our observation window or the relaxed cis isomer I_1 is formed directly from the excited state. At later delay times, when the excited-state absorption was gone, bleach signals at the blue edge were clearly resolved. The weak absorption tails at the red edge of the spectra are probably from solvated electrons due to two-photon ionization[8,19,64] of the chromophore. The pE46A experiment was also performed at pH 6.1, with almost identical results, as shown in Figure S2 (Supporting Information).

To illustrate the differences in excited-state decay dynamics, we show in Figure 5 decay traces recorded at 380 nm of the

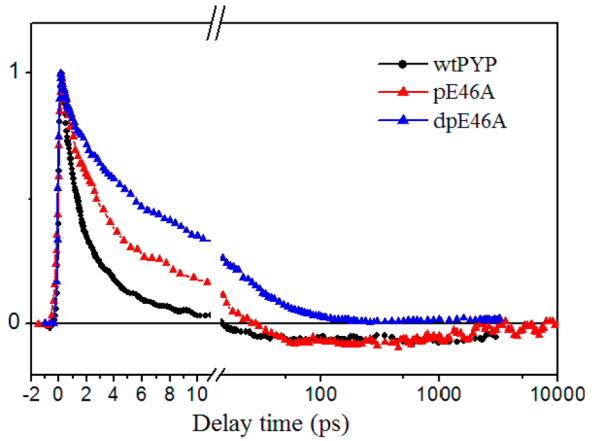

Figure 5. Excited-state decay dynamics at 380 nm for wtPYP, dpE46A, and pE46A. All three traces were normalized to their maximum amplitude.

three samples. In this wavelength region, strong excited-state absorption dominates the signals, and overlap with bleached ground-state absorption is minimal (see Figure 4). Therefore, the decay dynamics around this wavelength can be taken to roughly represent the pure excited-state dynamics. Comparison of the traces clearly shows that the excited-state decay of wtPYP is fastest, that of pE46A is slower with a significantly larger component in the tens of ps range, and that of dpE46A is even more so.

Global Fitting and Kinetic Model Target Analysis. *Sequential Schemes.* In order to fully describe the photoreaction dynamics for all samples, a global fitting analysis was performed, in which the full data set at all wavelengths was fitted to a minimal kinetic model and a convolution with an experimentally determined Gaussian instrument function was included. First, all samples were fitted to a sequential kinetic scheme as A → B → C → ···, which estimates the so-called "evolution associated difference spectra (EADSs)".[46−51]

The estimated EADSs for all three samples are shown in the three panels of Figure 6, respectively, along with the fitted time constants. Qualitatively, the EADSs were similar to the transient spectral shapes at selected delay times shown in Figure 4. Analyzed results for E46A at pH 6.0 and pH 9.3 are shown in Figure S3 (Supporting Information). The fitted time constant of each EADS was very different for the three samples. For wtPYP, five spectral exponents with decay times of 0.7, 2.2, 11.6, and 800 ps and a nondecaying component were needed, in good agreement with earlier reports.[6−12] For the dpE46A, also five spectral components, with decay times of 1.0, 6.2, 29, and 629 ps and a nondecaying component were required. For pE46A, only three spectral components could be extracted, consistent with the fact that the formation of only one photoisomerized product was observed.

To varying extents, these EADSs are mixtures of the involved excited and product states, and previous studies have demonstrated the applicability of a model involving up to three excited states, the I_0 and I_1 photoproduct states, and the GSI state.[6−12] To extract the pure species associated spectra (SAS) of these states and the relevant quantum yields, we

dx.doi.org/10.1021/jp506785q | J. Phys. Chem. B 2015, 119, 2372−2383

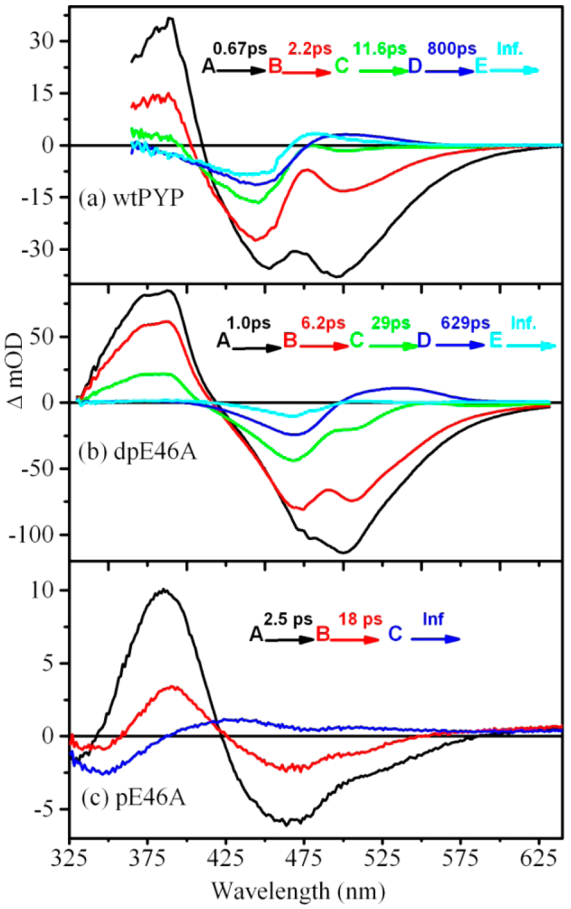

Figure 6. EADSs and decay time constants of wtPYP, dpE46A, and pE46A obtained by global fitting to a sequential decay model, as shown in the insets.

performed a further analysis with such a target kinetic model for the photoreaction in PYP.

Target Analysis. A detailed description of the target analysis method is included in the Supporting Information. The target analysis results for wtPYP are shown in Figure 7. Panel (a) presents the kinetic model and the rate constants from state to state (indicated as time constants). Three excited states E_1, E_2, and E_3 sequentially decaying from one to the other were needed to get a satisfactory fit of the experimental data. The ground-state bleach (GSB) was treated as a separate state, its concentration being equal to the sum of the concentrations of the excited, intermediate, and product states (cf. the olive curves in Figure 7B, F, and J). Its spectral shape was confined to the ground-state absorption spectrum, and its amplitude was freely adjusted during the fitting. The SAS in panel (c) show a physical and smooth spectral shape for each species and therefore satisfy an important criterion to evaluate the validity of the applied model. All of the SAS amplitudes are given in real extinction coefficient units of $(M\ cm)^{-1}$, which were scaled to the value of the extinction coefficient of the GSB (45500 M^{-1} cm^{-1} at 445 nm [2]). The population dynamics of all states are shown in panel (b). The GSI state had a lifetime of around 3.6 ps, and the excited states had a lifetime of 0.6, 2, and 13 ps, respectively. The quantum yield of the I_0 photoproduct was 32%, as can be calculated from the rate constants in (a) or by inspection of the population curve in (b). In this kind of analysis, the experimental observation of a species is described

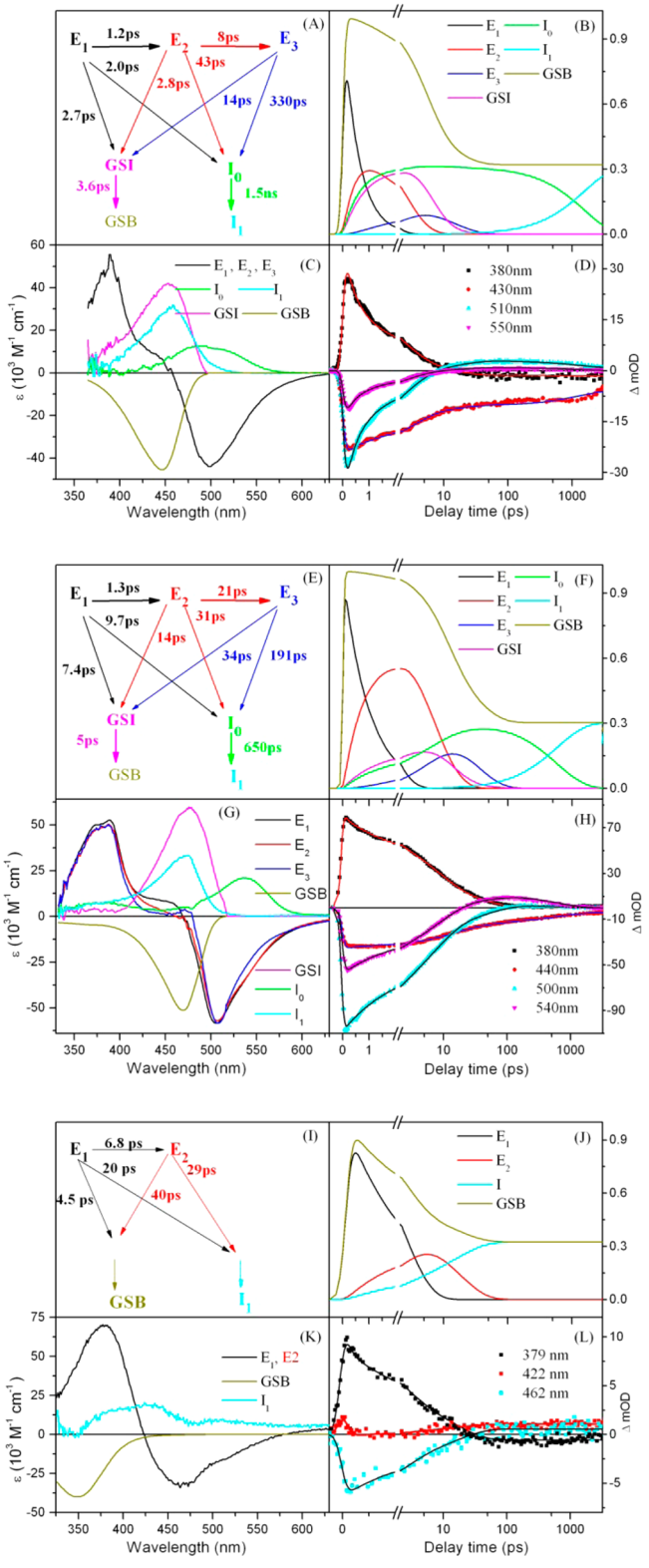

Figure 7. Target analysis of wtPYP (A–D), dpE46A (E–H), and pE46A (I–L). Kinetic model and fitted time constants (upper left panels). Fitted population decay of each species (upper right panels). Estimated SAS. The GSB spectrum is the inverted ground-state absorption spectrum that was used in the target analysis (lower left panels). Experimental decay traces with the corresponding fit at selected wavelengths (lower right panels).

dx.doi.org/10.1021/jp506785q | J. Phys. Chem. B 2015, 119, 2372–2383

Table 1. Excited-State Lifetimes and Quantum Yield of I_0 Formation for Each of the Three Excited States for wtPYP and E46A as Determined from the Target Analysis Depicted in Figure 7

	wt		dpE46A		pE46A	
sample	τ (ps)	QY	τ (ps)	QY	τ (ps)	QY
ES1	0.6	0.29	1	0.1	2.4	0.12
ES2	2	0.023	6.6	0.166	17	0.20
ES3	13	0.005	29	0.037		
total		0.32 ± 0.02		0.30 ± 0.02		0.32 ± 0.03

by the product of its population curve and its SAS. The crucial criterion in deciding whether these model parameters have been determined correctly is the relative size and shape of the SAS. As here the experimental ground-state spectrum was used as a separate spectral species in the fit, the size of the obtained I_0 and I_1 SAS can be compared directly to that of the GSB, making this criterion even stronger. According to Figure 7, the SAS have physically plausible shapes and amplitudes. In turn, this improves the reliability of the population curve and of the calculated quantum yields of I_0 and I_1. Note that a rougher estimate of the quantum yield can be obtained by comparing the ratios of the transient spectra directly; this produced similar values for the quantum yield; see the Supporting Information. For the dominant part, 29% of I_0 was formed from the first excited state and only 3% from the other excited states; see Table 1.

These target results for wtPYP compare well with those previously reported in vis−vis pump−(dump−)probe experiments.[7−9,11,12,65] In vis−IR pump−probe experiments, originally 2 or 3 ps time constants were reported for the excited-state decay in wtPYP in refs 10 and 15, respectively. In a later vis−IR study, performed with a higher S/N ratio, the GSI state was resolved, and a single 1.2 ps time constant was extracted for the excited-state decay in wtPYP.[6] Due to the intrinsically lower S/N in IR studies, it was not possible to resolve this single 1.2 ps into more components; therefore, this component was interpreted[6] as the average of the 0.6 and 2 ps components observed in vis−vis studies.

The use of the GSB as a separate spectral species in the fitting has as important advantage that true product state spectra are obtained, instead of product-minus-ground state absorption difference spectra, as discussed above. This now also allows us to compare the GSI absorption spectrum with those of the ground-state (pG) and of I_1. The GSI SAS have a shape very similar to the ground-state absorption, with a spectral shift of around 8 nm to the red. The spectrum of I_1 is shifted by ∼15 nm in comparison to that of the pG ground state. Finally, panel (d) presents decay traces at several selected wavelengths with the corresponding fit at that wavelength to show that the model fits the data over the full wavelength range. More experimental traces overlaid with the results of the fits obtained with the target modeling can be found in the Supporting Information, Figure S4.

Using the same kinetic target model, the dpE46A data were fitted. The obtained SAS and rate constants are presented in Figure 7E−H. The lifetime of the excited states was 1, 6.6, and 29 ps for E1, E2, and E3, respectively, and significantly longer than those of wtPYP, whereas the transition from I_0 to I_1 was two times faster with a 650 ps time constant. The lifetime of the GSI was found to be similar, 5 ps, as that in wtPYP. The quantum yield of the I_0 and I_1 product states was 30%; about 1/3 of the product formation occurred from E1, and about 1/2 was from E2. The SAS were also rescaled to the extinction coefficient value of the GSB (51100 M^{-1} cm^{-1} at 470 nm[42]). More fitted decay traces can be found in the Supporting Information, Figure S5. These results differ from those reported earlier for the E46A mutant by Devanathan et al;[66] fitted with a single exponential decay, they reported the dpE46A excited state to have a lifetime of 2.7 ps, while I_1 formation was reported to be 100-fold faster than that in wt, with a 40 ps time constant. Furthermore, a photochemical yield of 54% was reported.[66]

The high-quality of the dpE46A data allowed for resolving the spectral dynamics in the excited state, as ES1−3 could be estimated independently. This yielded the spectra (Figure 7G) to reveal a small red shift in 1 ps and a modest narrowing of the stimulated emission in 6.6 ps, consistent with the dynamics of wtPYP resolved in fluorescence upconversion experiments.[67−69] The narrowing has been ascribed to small-scale excited-state reorganization and vibrational relaxation of the molecule;[67−69] however, it could also reflect evolution along the twisting coordinate as locked variants of the chromophore lacked this spectral dynamics.[69]

In the pE46A target analysis (Figure 7I−L), four compartments were used, two for the excited state (having the same spectrum), a ground state, and an I_1 product state. Use of the ground-state absorption spectrum yielded again very good excited-state spectra displaying excited-state absorption peaking at 380 nm and stimulated emission at 470 nm. The product state spectrum is less well pronounced compared to the other samples, possibly due to a lower S/N of the data and peaks at around 435 nm. The SAS were also rescaled to the extinction coefficient value of the GSB (39900 M^{-1} cm^{-1} at 350 nm, determined from the E46A pH titration data in Figure S1, Supporting Information).

From a mathematical point of view, the data can be equally well described by a parallel model, in which the excited states decay independently, as by the sequential model used here, in which a short-lived excited state relaxes into the next-longer-living state, in line with earlier reports[6−12] (see ref 8 for an explicit comparison between the sequential and parallel model). In all cases, the spectra resolved for the excited states in sequential or parallel models were identical (apart from the small evolution in E46A), and the states differ only in their decay rate and productivity to form I_0. Therefore, up to now, it was unclear whether the different time constants and the different reactivities were representative of a relaxation process in the excited state (i.e., an evolution from a more toward a less productive minimum on the excited-state surface) or whether they were caused by heterogeneity or inhomogeneity due to small structural differences between individual protein molecules. In practice, when using a parallel kinetic scheme, the SAS of the excited states have to be equated in order to estimate them. With a sequential kinetic scheme, this is no longer needed, and thus, it allows us (given the very high S/N of the dpE46A data) to monitor the spectral evolution of the SAS of

dx.doi.org/10.1021/jp506785q | J. Phys. Chem. B 2015, 119, 2372−2383

the excited states. Deciding whether the parallel or the sequential kinetic scheme is the best physical description needs to be done on the basis of the estimated SAS that result from the analysis or "external" knowledge. The spectral evolution that we have resolved here for the first time in transient absorption data agrees with the spectral evolution observed in ultrafast emission data.[67−69] Furthermore, we checked whether an inhomogeneity toward product formation exists in the ground-state absorption spectrum by comparing experiments with different excitation wavelengths on wtPYP. In Figure S6 (Supporting Information), the decay traces upon excitation at 400 and 455 nm, recorded at a probe wavelength of 375 nm, are shown. Clearly, the excited-state decay dynamics are identical for both excitation wavelengths, confirming that there is no spectral inhomogeneity in PYP. It seems therefore that either the heterogeneity, described by three ESs, is a structural variance that does not affect the pCa absorption spectrum or that a relaxation process in the excited state toward a less productive minimum occurs. High-resolution X-ray diffraction studies have not revealed any indication for significant structural inhomogeneity,[30−32] though solution NMR data reported two conformations for R52.[70] Here, we conclude that most likely, the multiexponential decay of the pCa excited state in PYP is due to a relaxation on the excited-state potential energy surface, from a more to a less productive minimum in wtPYP, though a contribution from heterogeneity cannot be excluded.

DISCUSSION

We have investigated the roles of the short HBs between pCa, E46, and Y42 and of the negative charge stabilized by these HBs in the trans−cis isomerization process. We replaced E46 with alanine and measured the E46A mutant both in the pCa deprotonated and in the pCa protonated state. To analyze the actual structural changes induced by the E46A mutation, we performed MD simulations and analyzed steady-state spectroscopic characteristics of these three forms of PYP as no crystal structure for E46A-PYP is available yet.

The similar widths of the absorption and emission spectra indicate that the dpE46A protein provides a similarly restricted protein nanospace for the chromophore as in wtPYP. The MD results confirm that the lost HB of the pCa phenolic oxygen with E46 is replaced by a new HB with T50. The new HB with T50 is of close to normal length, whereas the HB with Y42 seems to have shortened in E46A. The shortening of the HB with Y42 is in good agreement with the observation of a strengthening of the HB with Y42 in the mutant E46Q by Sigala et al. with NMR.[63]However, the red shift in the E46A absorption spectrum indicates that the anionic character of the chromophore phenolate oxygen has increased.[37,38,62] Therefore, the new combination of HBs with T50 and Y42 leads to less stabilization of the negative charge on the phenolate oxygen and confirms the earlier suggested role of the short HB of E46 and Y42 in stabilization of the negative charge on the phenolate oxygen.[29] Interestingly, R52 mutants do not show such a red shift in the absorption, confirming that R52 does not play a role in the electrostatic interaction with the chromophore.[11,28,62]

How do these changes affect the isomerization rate and yield? In dpE46A, the yield is in effect the same as that in wtPYP, 30 ± 2 versus 32 ± 2%. The rate of isomerization is more dramatically affected; instead of a main 0.6 ps time constant, isomerization occurs with 1 and 6.6 ps time constants. QM/MM simulations[24−26] suggested the HBs of the phenolic oxygen to Y42 and E46 to be the crucial factor for the ultrafast decay from the twisted double-bond minimum. The HBs that the phenolic oxygen accepts from E46 and Y42 are very short. X-ray crystallographic studies of PYP with better than 1.0 Å resolution[30−32] revealed 2.5−2.6 Å oxygen−oxygen distances for the HBs donated by Y42 and E46, respectively. In principle, the pCa chromophore can twist and isomerize along both the C4−C7 and the C7═C8 bonds, depending on the charge redistribution in the chromophore. The stabilization of the double bond torsion was found to depend on the length of the Y42/E46 HBs.[25] Shorter HBs were suggested to significantly enhance the stabilization and again were proposed to be an important factor for the successful trans−cis isomerization of the chromophore in the native protein.[25] Our results confirm that indeed a lengthening of one of the HBs and a concomitant larger negative charge on the phenolic oxygen lead to a slower isomerization process but remarkably *not* a lower quantum yield.

When the charge density is varied quite strongly in the opposite direction, that is, a very low charge density in protonated E46A, no reduction in photochemical yield is observed. In the pCa protonated state, the protein enters the photocycle as a long-lived I_1-like intermediate is formed, with a quantum yield of 32 ± 3%, similar to that in wtPYP and dpE46A. Therefore, the further loss of the HBs with Y42 (and with T50) in pE46A and the large reduction in charge density on the phenolate oxygen do not reduce the chance for isomerization. We conclude therefore that the negative charge on the phenolate oxygen and the HBs that stabilize this charge have no effect on the quantum yield of isomerization, only on the rate of isomerization. The negative charge does play an important role later in the photocyle, where proton transfer from the side chain of Glu46 to the pCA creates a destabilizing buried charge on Glu46 that acts as an "electrostatic epicenter" and drives protein conformational changes during the activation of PYP.[20,71,72]

The variation in isomerization rate but constant isomerization quantum yield in the three different PYP proteins studied here can be understood within the framework of conical intersection used to describe isomerization mechanics.[73] Here, the multiphasic isomerization rates describe the evolution on the excited-state potential toward conical intersection, leading to the observed narrowing of the stimulated emission spectra, Figure 7G and refs 67−69. The exact geometry of the potential energy surfaces (PESs) at the conical intersection determines whether the chromophore isomerizes or falls back to the trans ground state (see Figure 8). In wtPYP, the lower quantum yield associated with the slower time constants may be due to a relaxation on the ES along a coordinate perpendicular to the isomerization coordinate, resulting in different time constants for reaching the conical intersection, in the case of wtPYP of 0.6, 2, and 13 ps. Crossing the conical intersection toward the cis PES or toward the trans ground state is characterized by a probability that describes the likelihood of a further evolution along the reaction coordinate, possibly determined by the breaking of the HB with the pCa carbonyl. Thus, the lifetime of the excited state is determined by how fast the conical intersection is reached, but the quantum yield is determined by the detailed geometry of the trans and cis ground state and ES PES at the conical intersection. The dpE46A and pE46A data can be described within the same framework of excited-state relaxation and competing crossing of the conical intersection

dx.doi.org/10.1021/jp506785q | J. Phys. Chem. B 2015, 119, 2372−2383

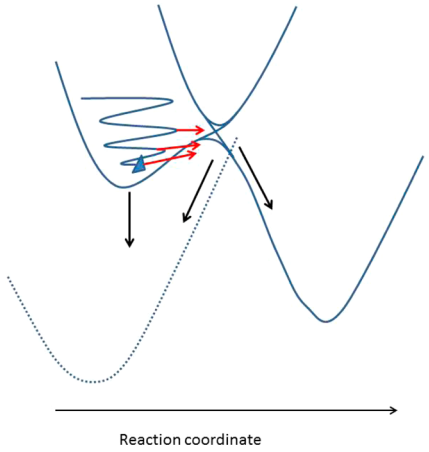

Figure 8. Potential energy surface of PYP as a function of the isomerization reaction coordinate. Dotted line: ground-state surface; upper left: excited-state surface, trans configuration; right: cis ground-state surface. The blue arrow indicates relaxation along a coordinate perpendicular to the reaction coordinate; red arrows are evolution toward conical intersection; black arrows indicate relaxation on trans and cis ground-state surfaces.

toward the cis PES or trans ground state. Interestingly, the slower rates but constant quantum yield for dpE46A and pE46A suggest that changes to the HB network with pCa phenolic oxygen affect only the evolution on the excited-state potential toward the conical intersection but not the dynamics at the conical intersection.

There are mutations that do lead to a lower isomerization quantum yield, such as T50V, with a reduction relative to the wt yield in the corresponding study to 71%, R52Q (61%),[9] R52A (79%),[11] P68V (95%), P68A (82%), and P68G (68%).[7] These are mutations that modify the HB network not near the pCa phenolic oxygen but further along the backbone of the chromophore, including the HB between the carbonyl group of the pCa and the backbone nitrogen atom of C69 in the P68 mutants.[7] This suggests that the residues around the backbone of the pCa molecule play a larger role in affecting an efficient isomerization than the negative charge of pCa and the short HBs stabilizing the negative charge. In PYP, owing to the spatial constraints imposed by the protein environment, isomerization proceeds via a volume-conserving mechanism through either the hula-twist (HT)[30,71−74] or bicycle-pedal (BP) mechanism.[74,75] In earlier work, we showed that a twist around the single bond helps the rotation around the double bond,[11] in agreement with QM/MM analysis.[25] Nevertheless, for isomerization, some structural changes to the protein surroundings need to occur; most notably, the HB between pCA and C69 needs to break, either before[6,23,30,76,77] or after isomerization.[74,75] In view of the obstructing role of the HB between the pCa carbonyl and C69, we speculate that one of the quantum-yield-determining events is the breaking of the pCa−C69 HB, enabling isomerization to occur. This rationalizes why mutations near the pCa carbonyl affect the isomerization quantum yield and mutations near the phenolic oxygen do not. Other key events may be concerted motions of P68, Y98, and the thioester linkage of the chromophore, deduced from B-factor analyses of a high-resolution pG structure, that is, a ground-state structure, suggested to facilitate the C═O flip during isomerization,[78] and to be essential for the functionality of the protein.

CONCLUSIONS

We have investigated how the excited-state and the photoisomerization dynamics of PYP are affected by the negative charge on the pCa chromophore and the short HBs with E46 and Y42 by MD simulations and ultrafast time-resolved spectroscopy. We have used the PYP mutant E46A at low and high pH to reduce the number of HBs between the phenolic oxygen of pCa and the protein and to vary the charge density. For the first time, we have studied the initial photoreaction of the protonated chromophore in PYP in the ultrafast time range and demonstrated it to be photoactive. We performed a target global analysis of time-resolved spectra using the ground-state absorption spectrum as an input. This provided us with true product state species absorption and stimulated emission spectra. The isomerization quantum yield in dpE46A was estimated to be 30 ± 2%, similar to wtPYP, and the excited-state lifetime was estimated to be longer by a factor of 2 in comparison with wtPYP. The photoreaction quantum yield of pE46A was around 32%, and while the excited-state lifetime became a little faster than that in dpE46A, it was still much slower than that of wtPYP. From these results, we conclude that the negative charge on pCa stabilized by the short HBs with E46 and Y42 affects the rate of isomerization but not the quantum yield of isomerization. We suggest that protein dynamics near the pCa backbone are important to accommodate the chromophore during isomerization and that these are a determining factor in the isomerization process.

ASSOCIATED CONTENT

Supporting Information

More data and details on the global target analysis method. This material is available free of charge via the Internet at http://pubs.acs.org.

AUTHOR INFORMATION

Corresponding Author

*E-mail: m.l.groot@vu.nl.

Author Contributions

The manuscript was written through contributions of all authors.

Notes

The authors declare no competing financial interest.

ACKNOWLEDGMENTS

This work was supported by the Dutch organization for scientific research NWO, through the division of Earth and Life Sciences (ALW), and through an Open Programme grant to M.L.G. and a Medium Large Investment grant to M.L.G. and K.J.H. M.H. was supported by a grant from the HFS Programme to K.J.H. J.V. acknowledges financial support from NWO (Athena grant). Gerrit Groenhof is acknowledged for providing force field parameters for the protonated and deprotonated chromophores.

ABBREVIATIONS

PYP, photoactive yellow protein; pCa, *p*-coumaric acid; wt, wild type; ps, picosecond; nm, nanometer; HB, hydrogen bond

REFERENCES

(1) Cusanovich, M. A.; Meyer, T. E. Photoactive yellow protein: a prototypic PAS domain sensory protein and development of a common signaling mechanism. *Biochemistry* **2003**, *42*, 4759.

(2) Meyer, T. E.; Tollin, G.; Hazzard, J. H.; Cusanovich, M. A. Photoactive yellow protein from the purple phototrophic bacterium, Ectothiorhodospira halophila. Quantum yield of photobleaching and effects of temperature, alcohols, glycerol, and sucrose on kinetics of photobleaching and recovery. *Biophys. J.* **1989**, *56*, 559.
(3) Sprenger, W. W.; Hoff, W. D.; Armitage, J. P.; Hellingwerf, K. J. The eubacterium Ectothiorhodospira halophila is negatively phototactic, with a wavelength dependence that fits the absorption spectrum of the photoactive yellow protein. *J. Bacteriol.* **1993**, *175*, 3096.
(4) van Brederode, M. E.; Gensch, T.; Hoff, W. D.; Hellingwerf, K. J.; Braslavsky, S. E. Photoinduced volume change and energy storage associated with the early transformations of the photoactive yellow protein from Ectothiorhodospira halophila. *Biophys. J.* **1995**, *68*, 1101.
(5) Gensch, T.; Hellingwerf, K. J.; Braslavsky, S. E.; Schaffner, K. Photoequilibrium in the primary steps of the photoreceptors phytochrome A and photoactive yellow protein. *J. Phys. Chem. A* **1998**, *102*, 5398.
(6) van Wilderen, L. J.; van der Horst, M. A.; van Stokkum, I. H.; Hellingwerf, K. J.; van Grondelle, R.; Groot, M. L. Ultrafast infrared spectroscopy reveals a key step for successful entry into the photocycle for photoactive yellow protein. *Proc. Natl. Acad. Sci. U.S.A.* **2006**, *103*, 15050.
(7) Rupenyan, A. B.; Vreede, J.; van Stokkum, I. H.; Hospes, M.; Kennis, J. T.; Hellingwerf, K. J.; Groot, M. L. Proline 68 enhances photoisomerization yield in photoactive yellow protein. *J. Phys. Chem. B* **2011**, *115*, 6668.
(8) Larsen, D. S.; van Stokkum, I. H.; Vengris, M.; van Der Horst, M. A.; de Weerd, F. L.; Hellingwerf, K. J.; van Grondelle, R. Incoherent manipulation of the photoactive yellow protein photocycle with dispersed pump−dump−probe spectroscopy. *Biophys. J.* **2004**, *87*, 1858.
(9) Changenet-Barret, P.; Plaza, P.; Martin, M. M.; Chosrowjan, H.; Taniguchi, S.; Mataga, N.; Imamoto, Y.; Kataoka, M. Structural Effects on the Ultrafast Photoisomerization of Photoactive Yellow Protein. Transient Absorption Spectroscopy of Two Point Mutants. *J. Phys. Chem. C* **2009**, *113*, 11605.
(10) Groot, M. L.; van Wilderen, L. J.; Larsen, D. S.; van der Horst, M. A.; van Stokkum, I. H.; Hellingwerf, K. J.; van Grondelle, R. Initial steps of signal generation in photoactive yellow protein revealed with femtosecond mid-infrared spectroscopy. *Biochemistry* **2003**, *42*, 10054.
(11) Stahl, A. D.; Hospes, M.; Singhal, K.; van Stokkum, I.; van Grondelle, R.; Groot, M. L.; Hellingwerf, K. J. On the Involvement of Single-Bond Rotation in the Primary Photochemistry of Photoactive Yellow Protein. *Biophys. J.* **2011**, *101*, 1184.
(12) Lincoln, C. N.; Fitzpatrick, A. E.; van Thor, J. J. Photoisomerisation quantum yield and non-linear cross-sections with femtosecond excitation of the photoactive yellow protein. *Phys. Chem. Chem. Phys.* **2012**, *14*, 15752.
(13) Ujj, L.; Devanathan, S.; Meyer, T. E.; Cusanovich, M. A.; Tollin, G.; Atkinson, G. H. New photocycle intermediates in the photoactive yellow protein from Ectothiorhodospira halophila: picosecond transient absorption spectroscopy. *Biophys. J.* **1998**, *75*, 406.
(14) Devanathan, S.; Pacheco, A.; Ujj, L.; Cusanovich, M.; Tollin, G.; Lin, S.; Woodbury, N. Femtosecond spectroscopic observations of initial intermediates in the photocycle of the photoactive yellow protein from Ectothiorhodospira halophila. *Biophys. J.* **1999**, *77*, 1017.
(15) Heyne, K.; Mohammed, O. F.; Usman, A.; Dreyer, J.; Nibbering, E. T. J.; Cusanovich, M. A. Structural evolution of the chromophore in the primary stages of trans/cis isomerization in photoactive yellow protein. *J. Am. Chem. Soc.* **2005**, *127*, 18100.
(16) Hellingwerf, K. J.; Hendriks, J.; Gensch, T. Photoactive Yellow Protein, a new type of photoreceptor protein: Will this "yellow lab" bring us where we want to go? *J. Phys. Chem. A* **2003**, *107*, 1082.
(17) Larsen, D. S.; van Grondelle, R. Initial photoinduced dynamics of the photoactive yellow protein. *ChemPhysChem* **2005**, *6*, 828.
(18) Changenet-Barret, P.; Espagne, A.; Plaza, P.; Hellingwerf, K. J.; Martin, M. M. Investigations of the primary events in a bacterial photoreceptor for photomotility: photoactive yellow protein (PYP). *New J. Chem.* **2005**, *29*, 527.
(19) Larsen, D. S.; Vengris, M.; van Stokkum, I. H.; van der Horst, M. A.; de Weerd, F. L.; Hellingwerf, K. J.; van Grondelle, R. Photoisomerization and photoionization of the photoactive yellow protein chromophore in solution. *Biophys. J.* **2004**, *86*, 2538.
(20) Xie, A.; Hoff, W. D.; Kroon, A. R.; Hellingwerf, K. J. Glu46 donates a proton to the 4-hydroxycinnamate anion chromophore during the photocycle of photoactive yellow protein. *Biochemistry* **1996**, *35*, 14671.
(21) Imamoto, Y.; Mihara, K.; Hisatomi, O.; Kataoka, M.; Tokunaga, F.; Bojkova, N.; Yoshihara, K. Evidence for proton transfer from Glu-46 to the chromophore during the photocycle of photoactive yellow protein. *J. Biol. Chem.* **1997**, *272*, 12905.
(22) Premvardhan, L. L.; van der Horst, M. A.; Hellingwerf, K. J.; van Grondelle, R. Stark spectroscopy on photoactive yellow protein, E46Q, and a nonisomerizing derivative, probes photo-induced charge motion. *Biophys. J.* **2003**, *84*, 3226.
(23) Groenhof, G.; Bouxin-Cademartory, M.; Hess, B.; De Visser, S. P.; Berendsen, H. J.; Olivucci, M.; Mark, A. E.; Robb, M. A. Photoactivation of the photoactive yellow protein: why photon absorption triggers a trans-to-cis isomerization of the chromophore in the protein. *J. Am. Chem. Soc.* **2004**, *126*, 4228.
(24) Gromov, E. V.; Burghardt, I.; Hynes, J. T.; Koppel, H.; Cederbaum, L. S. Electronic structure of the photoactive yellow protein chromophore: Ab initio study of the low-lying excited singlet states. *J. Photochem. Photobiol., A* **2007**, *190*, 241.
(25) Gromov, E. V.; Burghardt, I.; Koppel, H.; Cederbaum, L. S. Native hydrogen bonding network of the photoactive yellow protein (PYP) chromophore: Impact on the electronic structure and photoinduced isomerization. *J. Photochem. Photobiol., A* **2012**, *234*, 123.
(26) Boggio-Pasqua, M.; Robb, M. A.; Groenhof, G. Hydrogen Bonding Controls Excited-State Decay of the Photoactive Yellow Protein Chromophore. *J. Am. Chem. Soc.* **2009**, *131*, 13580.
(27) Borgstahl, G. E.; Williams, D. R.; Getzoff, E. D. 1.4 A structure of photoactive yellow protein, a cytosolic photoreceptor: unusual fold, active site, and chromophore. *Biochemistry* **1995**, *34*, 6278.
(28) Changenet-Barret, P.; Plaza, P.; Martin, M. M.; Chosrowjan, H.; Taniguchi, S.; Mataga, N.; Imamoto, Y.; Kataoka, M. Role of arginine 52 on the primary photoinduced events in the PYP photocycle. *Chem. Phys. Lett.* **2007**, *434*, 320.
(29) Yamaguchi, S.; Kamikubo, H.; Kurihara, K.; Kuroki, R.; Niimura, N.; Shimizu, N.; Yamazaki, Y.; Kataoka, M. Low-barrier hydrogen bond in photoactive yellow protein. *Proc. Natl. Acad. Sci. U.S.A.* **2009**, *106*, 440.
(30) Genick, U. K.; Soltis, S. M.; Kuhn, P.; Canestrelli, I. L.; Getzoff, E. D. Structure at 0.85 A resolution of an early protein photocycle intermediate [see comments]. *Nature* **1998**, *392*, 206.
(31) Getzoff, E. D.; Gutwin, K. N.; Genick, U. K. Anticipatory active-site motions and chromophore distortion prime photoreceptor PYP for light activation. *Nat. Struct. Biol.* **2003**, *10*, 663.
(32) Fisher, S. Z.; Anderson, S.; Henning, R.; Moffat, K.; Langan, P.; Thiyagarajan, P.; Schultz, A. J. Neutron and X-ray structural studies of short hydrogen bonds in photoactive yellow protein (PYP). *Acta Crystallogr., Sect. D* **2007**, *63*, 1178.
(33) Kumauchi, M.; Hara, M. T.; Stalcup, P.; Xie, A. H.; Hoff, W. D. Identification of six new photoactive yellow proteins — Diversity and structure−function relationships in a bacterial blue light photoreceptor. *Photochem. Photobiol.* **2008**, *84*, 956.
(34) Mataga, N.; Chosrowjan, H.; Shibata, Y.; Imamoto, Y.; Tokunaga, F. Effects of modification of protein nanospace structure and change of temperature on the femtosecond to picosecond fluorescence dynamics of photoactive yellow protein. *J. Phys. Chem. B* **2000**, *104*, 5191.
(35) Devanathan, S.; Lin, S.; Cusanovich, M. A.; Woodbury, N.; Tollin, G. Early photocycle kinetic behavior of the E46A and Y42F mutants of photoactive yellow protein: Femtosecond spectroscopy. *Biophys. J.* **2001**, *81*, 2314.
(36) Brudler, R.; Meyer, T. E.; Genick, U. K.; Devanathan, S.; Woo, T. T.; Millar, D. P.; Gerwert, K.; Cusanovich, M. A.; Tollin, G.;

Getzoff, E. D. Coupling of hydrogen bonding to chromophore conformation and function in photoactive yellow protein. *Biochemistry* **2000**, *39*, 13478.
(37) Philip, A. F.; Eisenman, K. T.; Papadantonakis, G. A.; Hoff, W. D. Functional Tuning of Photoactive Yellow Protein by Active Site Residue 46. *Biochemistry* **2008**, *47*, 13800.
(38) Devanathan, S.; Brudler, R.; Hessling, B.; Woo, T. T.; Gerwert, K.; Getzoff, E. D.; Cusanovich, M. A.; Tollin, G. Dual photoactive species in Glu46Asp and Glu46Ala mutants of photoactive yellow protein: a pH-driven color transition. *Biochemistry* **1999**, *38*, 13766.
(39) Kroon, A. R.; Hoff, W. D.; Fenneman, H. P. M.; Gijzen, J.; Koomen, G. J.; Verhoeven, J. W.; Crielaard, W.; Hellingwerf, K. J. Spectral tuning, fluorescence, and photoactivity in hybrids of photoactive yellow protein, reconstituted with native or modified chromophores. *J. Biol. Chem.* **1996**, *271*, 31949.
(40) Hoff, W. D.; Van Stokkum, I. H. M.; Gural, J.; Hellingwerf, K. J. Comparison of acid denaturation and light activation in the eubacterial blue-light receptor photoactive yellow protein. *Biochim. Biophys. Acta, Bioenerg.* **1997**, *1322*, 151.
(41) Meyer, T. E.; Devanathan, S.; Woo, T.; Getzoff, E. D.; Tollin, G.; Cusanovich, M. A. Site-specific mutations provide new insights into the origin of pH effects and alternative spectral forms in the photoactive yellow protein from *Halorhodospira halophila*. *Biochemistry* **2003**, *42*, 3319.
(42) Imamoto, Y.; Koshimizu, H.; Mihara, K.; Hisatomi, O.; Mizukami, T.; Tsujimoto, K.; Kataoka, M.; Tokunaga, F. Roles of amino acid residues near the chromophore of photoactive yellow protein. *Biochemistry* **2001**, *40*, 4679.
(43) van Aalten, D. M.; Haker, A.; Hendriks, J.; Hellingwerf, K. J.; Joshua-Tor, L.; Crielaard, W. Engineering photocycle dynamics. Crystal structures and kinetics of three photoactive yellow protein hinge-bending mutants. *J. Biol. Chem.* **2002**, *277*, 6463.
(44) Kort, R.; Hoff, W. D.; Van West, M.; Kroon, A. R.; Hoffer, S. M.; Vlieg, K. H.; Crielaand, W.; Van Beeumen, J. J.; Hellingwerf, K. J. The xanthopsins: a new family of eubacterial blue-light photoreceptors. *EMBO J.* **1996**, *15*, 3209.
(45) Hendriks, J.; Gensch, T.; Hviid, L.; van Der Horst, M. A.; Hellingwerf, K. J.; van Thor, J. J. Transient exposure of hydrophobic surface in the photoactive yellow protein monitored with Nile Red. *Biophys. J.* **2002**, *82*, 1632.
(46) van Stokkum, I. H.; Larsen, D. S.; van Grondelle, R. Global and target analysis of time-resolved spectra. *Biochim. Biophys. Acta* **2004**, *1657*, 82.
(47) Ernsting, N. P.; Kovalenko, S. A.; Senyushkina, T.; Saam, J.; Farztdinov, V. Wave-packet-assisted decomposition of femtosecond transient ultraviolet−visible absorption spectra: Application to excited-state intramolecular proton transfer in solution. *J. Phys. Chem. A* **2001**, *105*, 3443.
(48) Cong, H.; Niedzwiedzki, D. M.; Gibson, G. N.; Frank, H. A. Ultrafast time-resolved spectroscopy of xanthophylls at low temperature. *J. Phys. Chem. B* **2008**, *112*, 3558.
(49) Zhu, J. Y.; Gdor, I.; Smolensky, E.; Friedman, N.; Sheves, M.; Ruhman, S. Photoselective Ultrafast Investigation of Xanthorhodopsin and Its Carotenoid Antenna Salinixanthin. *J. Phys. Chem. B* **2010**, *114*, 3038.
(50) van Wilderen, L. J.; Lincoln, C. N.; van Thor, J. J. Modelling multi-pulse population dynamics from ultrafast spectroscopy. *PLoS One* **2011**, *6*, e17373.
(51) Snellenburg, J. J.; Laptenok, S. P.; Seger, R.; Mullen, K. M.; van Stokkum, I. H. M. Glotaran: A Java-Based Graphical User Interface for the R Package TIMP. *J. Stat. Software* **2012**, *49*, 1.
(52) Pronk, S.; Pall, S.; Schulz, R.; Larsson, P.; Bjelkmar, P.; Apostolov, R.; Shirts, M. R.; Smith, J. C.; Kasson, P. M.; van der Spoel, D.; Hess, B.; Lindahl, E. GROMACS 4.5: a high-throughput and highly parallel open source molecular simulation toolkit. *Bioinformatics* **2013**, *29*, 845.
(53) Hess, B.; Kutzner, C.; van der Spoel, D.; Lindahl, E. GROMACS 4: Algorithms for highly efficient, load-balanced, and scalable molecular simulation. *J. Chem. Theory Comput.* **2008**, *4*, 435.
(54) Duan, Y.; Wu, C.; Chowdhury, S.; Lee, M. C.; Xiong, G. M.; Zhang, W.; Yang, R.; Cieplak, P.; Luo, R.; Lee, T.; Caldwell, J.; Wang, J. M.; Kollman, P. A point-charge force field for molecular mechanics simulations of proteins based on condensed-phase quantum mechanical calculations. *J. Comput. Chem.* **2003**, *24*, 1999.
(55) Mahoney, M. W.; Jorgensen, W. L. A five-site model for liquid water and the reproduction of the density anomaly by rigid, nonpolarizable potential functions. *J. Chem. Phys.* **2000**, *112*, 8910.
(56) Bussi, G.; Donadio, D.; Parrinello, M. Canonical sampling through velocity rescaling. *J. Chem. Phys.* **2007**, *126*, 014101.
(57) Parrinello, M.; Rahman, A. Polymorphic Transitions in Single-Crystals — A New Molecular-Dynamics Method. *J. Appl. Phys.* **1981**, *52*, 7182.
(58) Darden, T.; York, D.; Pedersen, L. Particle Mesh Ewald - An N·log(N) Method for Ewald Sums in Large Systems. *J. Chem. Phys.* **1993**, *98*, 10089.
(59) Essmann, U.; Perera, L.; Berkowitz, M. L.; Darden, T.; Lee, H.; Pedersen, L. G. A Smooth Particle Mesh Ewald Method. *J. Chem. Phys.* **1995**, *103*, 8577.
(60) Hess, B.; Bekker, H.; Berendsen, H. J. C.; Fraaije, J. G. E. M. LINCS: A linear constraint solver for molecular simulations. *J. Comput. Chem.* **1997**, *18*, 1463.
(61) Miyamoto, S.; Kollman, P. A. Settle — An Analytical Version of the Shake and Rattle Algorithm for Rigid Water Models. *J. Comput. Chem.* **1992**, *13*, 952.
(62) Genick, U. K.; Devanathan, S.; Meyer, T. E.; Canestrelli, I. L.; Williams, E.; Cusanovich, M. A.; Tollin, G.; Getzoff, E. D. Active site mutants implicate key residues for control of color and light cycle kinetics of photoactive yellow protein. *Biochemistry* **1997**, *36*, 8.
(63) Sigala, P. A.; Tsuchida, M. A.; Herschlag, D. Hydrogen bond dynamics in the active site of photoactive yellow protein. *Proc. Natl. Acad. Sci. U.S.A.* **2009**, *106*, 9232.
(64) Zhu, J.; Paparelli, L.; Hospes, M.; Arents, J.; Kennis, J. T.; van Stokkum, I. H.; Hellingwerf, K. J.; Groot, M. L. Photoionization and electron radical recombination dynamics in photoactive yellow protein investigated by ultrafast spectroscopy in the visible and near-infrared spectral region. *J. Phys. Chem. B* **2013**, *117*, 11042.
(65) Carroll, E. C.; Hospes, M.; Valladares, C.; Hellingwerf, K. J.; Larsen, D. S. Is the photoactive yellow protein a UV-B/blue light photoreceptor? *Photochem. Photobiol. Sci.* **2011**, *10*, 464.
(66) Devanathan, S.; Lin, S.; Cusanovich, M. A.; Woodbury, N.; Tollin, G. Early photocycle kinetic behavior of the E46A and Y42F mutants of photoactive yellow protein: femtosecond spectroscopy. *Biophys. J.* **2001**, *81*, 2314.
(67) Hanada, H.; Kanematsu, Y.; Kinoshita, S.; Kumauchi, M.; Sasaki, J.; Tokunaga, F. Ultrafast fluorescence spectroscopy of photoactive yellow protein. *J. Lumin.* **2001**, *94*, 593.
(68) Changenet, P.; Zhang, H.; van der Meer, M. J.; Hellingwerf, K. J.; Glasbeek, M. Subpicosecond fluorescence upconversion measurements of primary events in yellow proteins. *Chem. Phys. Lett.* **1998**, *282*, 276.
(69) Vengris, M.; van der Horst, M. A.; Zgrablic, G.; van Stokkum, I. H. M.; Haacke, S.; Chergui, M.; Hellingwerf, K. J.; van Grondelle, R.; Larsen, D. S. Contrasting the excited-state dynamics of the photoactive yellow protein chromophore: Protein versus solvent environments. *Biophys. J.* **2004**, *87*, 1848.
(70) Dux, P.; Rubinstenn, G.; Vuister, G. W.; Boelens, R.; Mulder, F. A. A.; Hard, K.; Hoff, W. D.; Kroon, A. R.; Crielaard, W.; Hellingwerf, K. J.; Kaptein, R. Solution structure and backbone dynamics of the photoactive yellow protein. *Biochemistry* **1998**, *37*, 12689.
(71) Xie, A. H.; Kelemen, L.; Hendriks, J.; White, B. J.; Hellingwerf, K. J.; Hoff, W. D. Formation of a new buried charge drives a large-amplitude protein quake in photoreceptor activation. *Biochemistry* **2001**, *40*, 1510.
(72) Derix, N. M.; Wechselberger, R. W.; van der Horst, M. A.; Hellingwerf, K. J.; Boelens, R.; Kaptein, R.; van Nuland, N. A. J. Lack of negative charge in the E46Q mutant of photoactive yellow protein prevents partial unfolding of the blue-shifted intermediate. *Biochemistry* **2003**, *42*, 14501.

(73) Levine, B. G.; Martinez, T. J. Isomerization through conical intersections. *Annu. Rev. Phys. Chem.* **2007**, *58*, 613.
(74) Jung, Y. O.; Lee, J. H.; Kim, J.; Schmidt, M.; Moffat, K.; Šrajer, V.; Ihee, H. Volume-conserving trans−cis isomerization pathways in photoactive yellow protein visualized by picosecond X-ray crystallography. *Nat. Chem.* **2013**, *5*, 212.
(75) Schotte, F.; Cho, H. S.; Kaila, V. R. I.; Kamikubo, H.; Dashdorj, N.; Henry, E. R.; Graber, T. J.; Henning, R.; Wulff, M.; Hummer, G.; Kataoka, M.; Anfinrud, P. A. Watching a signaling protein function in real time via 100-ps time-resolved Laue crystallography. *Proc. Natl. Acad. Sci. U.S.A.* **2012**, *109*, 19256.
(76) Groenhof, G.; Lensink, M. F.; Berendsen, H. J. C.; Snijders, J. G.; Mark, A. E. Signal transduction in the photoactive yellow protein. I. Photon absorption and the isomerization of the chromophore. *Proteins: Struct. Funct. Bioinform.* **2002**, *48*, 202.
(77) Kort, R.; Hellingwerf, K. J.; Ravelli, R. B. G. Initial events in the photocycle of photoactive yellow protein. *J. Biol. Chem.* **2004**, *279*, 26417.
(78) Coureux, P. D.; Fan, Z. P.; Stojanoff, V.; Genick, U. K. Picometer-scale conformational heterogeneity separates functional from nonfunctional states of a photoreceptor protein. *Structure* **2008**, *16*, 863.